Regimes of two-color light bullet formation in a gradient waveguide

Sergey V. Sazonov*
National Research Centre "Kurchatov Institute", 1 Akademika Kurchatova Square, Moscow 123182, Russia

Aleksey A. Kalinovich, Maria V. Komissarova, and Irina G. Zakharova
Department of Photonics and Microwave Physics, Lomonosov Moscow State University, 1-2 Leninskie Gory, Moscow 119991, Russia

(Received 16 July 2019; published 26 September 2019)

In this paper we concentrate on the remarkable role of a gradient waveguide in two-color light bullet formation. We study generation of the second harmonic in such an inhomogeneous nonlinear medium, taking into account diffraction and relatively weak temporal dispersion. Using the averaged Lagrangian method we consider all possible combinations of the range of group velocities (normal or anomalous dispersion) and waveguide geometry (focusing or defocusing waveguide). Stability conditions for a propagating two-color light bullet are derived analytically. We demonstrate the formation of a stable two-component light bullet in a parabolic planar quadratically nonlinear waveguide either at anomalous or at normal group velocity dispersion. We discuss also the results of numerical simulation confirming our analytical findings. Besides that, simulation allows us to expand the scope of the study and to show light bullet propagation at a certain phase mismatching and the formation of a stable coupled localized structure from a signal at the fundamental frequency as well.

DOI: 10.1103/PhysRevA.100.033835

I. INTRODUCTION

It is well known that medium inhomogeneity influences greatly the formation and stability of optical solitons [1]. While longitudinal homogeneity manifests itself in photonic crystals and results in soliton trapping in the forbidden band gap (gap solitons) [1–5], transverse inhomogeneity plays an important role for soliton stabilization. This effect is known, for instance, in Bose-Einstein condensates: waveguides with both cubic and quadratic nonlinearities [1,6–9]. Introducing waveguide geometry, we can diversify a range of input parameters for which solitons may be observed.

If we deal with multidimensional light bullets, we have to notice that they are highly unstable in a homogeneous medium with Kerr nonlinearity. However, going to an inhomogeneous Kerr medium, where the linear part of the refraction index depends on transverse coordinates, one can prevent wave collapse. The interplay between dispersion, diffraction, index inhomogeneity, and Kerr nonlinearity is considered in detail in [1–10]. Anomalous group velocity dispersion (GVD) and infrared (IR) range seem to be natural choices for light bullet generation. At the same time, researchers have been showing interest in other frequency ranges, where the dispersion is normal, since the first studies of temporal and spatiotemporal solitons at the end of the 1990s [1,11]. At normal dispersion we have to compensate for spatial and temporal spreading. Nonlinearity may be rather weak; therefore, one should draw on additional factors which are able to compress the pulse. Using a waveguide seems to be promising to this end.

Recently we developed a detailed theory of "breathing" light bullets propagating in a quadratic nonlinear medium with anomalous dispersion [12,13]. Provided that the phase- and group-matching conditions hold and the second harmonic GVD coefficient is twice as large as the GVD coefficient for the fundamental wave, the averaged Lagrangian (AL) method allowed us to obtain an analytical solution in the form of a two-component spatiotemporal soliton. It was demonstrated that the above conditions can be fulfilled simultaneously in a microdispersive (granulated) medium in the THz range.

Continuing our investigations with microdispersive media [12,13], we initiated studies of light bullets in a planar waveguide at quadratic nonlinearity [14]. In the last of the mentioned works we developed a model of the second harmonic generation (SHG) in a gradient waveguide, taking into account diffraction and relatively weak temporal dispersion. Using a "slowly varying envelope approximation" and neglecting the dispersion of the nonlinear part of the response of the medium, we introduced a system of parabolic equations for the envelopes of both harmonics. We also derived integrals of motion of this system. To solve it numerically we constructed a nonlinear finite-difference scheme based on the Crank-Nicolson method preserving the integrals. Considering a parabolic waveguide profile, we demonstrated a competition between nonlinearity, dispersion, diffraction, and waveguide properties in numerical experiments. The most remarkable result concerns the observation of a stable two-component light bullet at normal dispersion. At the same time a lack of analytical criteria did not allow us to find out the limits of the bullet's existence. In the present work we deal with the model introduced in [14]. Similarly to [12,13], we apply the AL method and examine both anomalous and normal dispersion influence. We reveal analytically different regimes of spatial-temporal pulse propagation in a waveguide with quadratic nonlinearity.

*sazonov.sergey@gmail.com

Following the approach of [12], we derive a dynamic (z-dependent) solution in the form of a spatiotemporal soliton at the phase- and group-matching conditions. Moreover, we obtain stability conditions and periods of small oscillations of light bullet parameters depending on waveguide geometry and dispersion type (normal or anomalous). Numerical simulation shows the robust propagation of the analytically predicted wave with a period of intensity oscillations close to that theoretically derived. We also numerically study the dynamics of a two-color spatiotemporal soliton forming at SHG when the phase- and group-velocity-matching conditions are broken.

The paper is organized as follows. In Sec. II we apply the AL method to the system of equations describing SHG in a planar parabolic waveguide and obtain a soliton solution in the form of a light bullet at both fundamental and second frequencies. Analytical solutions and stability analysis are given in Sec. III. Results of direct numerical simulation are discussed in Sec. IV. We demonstrate a robust propagation of the derived solution in different regimes. Then, we show a possibility of two-component soliton formation when launching only the fundamental pulse into the medium, and we discuss the physical situation in which the phase matching conditions are violated. Section V contains the conclusions arising from the study.

II. METHOD OF AVERAGED LAGRANGIAN AND MODIFIED GROSS-PITAEVSKII EQUATION

As mentioned above, recently we developed a governing system of equations for SHG in a bulk waveguide with transverse inhomogeneity [14]. In this paper, we confine ourselves to an analysis of the propagation of a quasimonochromatic pulse in a planar waveguide. For a planar waveguide with arbitrary profile of the refractive index, the resulting system for the envelopes of the fundamental and second harmonics, taking into account the mutual influence of nonlinearity, planar diffraction, and weak temporal dispersion, is written as

$$\begin{aligned} i\left(\frac{\partial\Phi_1}{\partial z}+\delta\frac{\partial\Phi_1}{\partial\tau}\right) &= \omega q_1\Phi_1-\frac{\beta_\omega}{2}\frac{\partial^2\Phi_1}{\partial\tau^2} \\ &\quad +\alpha_\omega\Phi_1^*\Phi_2 e^{i(2k_1-k_2)z}+\frac{c}{2\omega n_\omega^{(0)}}\frac{\partial^2\Phi_1}{\partial x^2}, \\ i\left(\frac{\partial\Phi_2}{\partial z}-\delta\frac{\partial\Phi_2}{\partial\tau}\right) &= 2\omega q_2\Phi_2-\frac{\beta_{2\omega}}{2}\frac{\partial^2\Phi_2}{\partial\tau^2} \\ &\quad +\alpha_{2\omega}\Phi_1^2 e^{-i(2k_1-k_2)z}+\frac{c}{4\omega n_{2\omega}^{(0)}}\frac{\partial^2\Phi_2}{\partial x^2}. \end{aligned} \tag{1}$$

In (1) Φ_1 and Φ_2 are the slowly varying envelopes of both harmonics, ω is the fundamental carrier frequency of the input pulse, $k_1=k(\omega)$ and $k_2=k(2\omega)$ are the wave numbers, corresponding to the fundamental frequency ω and second harmonic 2ω, respectively, and

$$q_1=\frac{2\pi}{cn_\omega^{(0)}}\chi_\omega^{(0)}f_\omega,\quad q_2=\frac{2\pi}{cn_{2\omega}^{(0)}}\chi_{2\omega}^{(0)}f_{2\omega}. \tag{2}$$

c is the speed of light in vacuum and $\chi_{\omega,2\omega}^{(0)}$ are the linear susceptibilities of the medium at the center of the waveguide cross section. $f_\omega(x)$ and $f_{2\omega}(x)$ are the dimensionless functions satisfying the condition $f_\omega(0)=f_{2\omega}(0)=0$. $n_{\omega,2\omega}^{(0)}=\sqrt{1+4\pi\chi_{\omega,2\omega}^{(0)}}$ are the refractive indices of the frequencies ω and 2ω at the center of the waveguide cross section, and $\delta=\frac{1}{2}((v_g^{(\omega)})^{-1}-(v_g^{(2\omega)})^{-1})$ is the mismatch of group velocities, where the group velocities $v_g^{(\omega,2\omega)}$ at the center of the waveguide are defined as follows:

$$\frac{1}{v_g^{(\omega,2\omega)}}=\frac{\partial k}{\partial\omega}=\frac{1}{c}\left(n_{\omega,2\omega}^{(0)}+\omega\frac{\partial n_{\omega,2\omega}^{(0)}}{\partial\omega}\right).$$

In (1) we also denote the parameters of GVD as

$$\begin{aligned} \beta_\omega &= \frac{\partial^2k_1}{\partial\omega^2}=\frac{1}{c}\frac{\partial^2}{\partial\omega^2}(n_\omega\omega) \\ &= \frac{4\pi}{cn_\omega^{(0)}}\left[\frac{\partial\chi_\omega^{(0)}}{\partial\omega}+\frac{\omega}{2}\frac{\partial^2\chi_\omega^{(0)}}{\partial\omega^2}-\frac{\omega}{4\pi}\left(\frac{\partial n_\omega^{(0)}}{\partial\omega}\right)^2\right], \\ \beta_{2\omega} &= \frac{\partial^2k_2}{\partial(2\omega)^2}=(\beta_{\omega_1})_{\omega_1=2\omega}. \end{aligned}$$

$\alpha_\omega=2\pi\omega\chi^{(2)}(2\omega,-\omega)/(cn_\omega^{(0)})$ and $\alpha_{2\omega}=4\pi\chi^{(2)}(\omega,\omega)\omega/(cn_{2\omega}^{(0)})$ are the nonlinear parameters, and $\chi^{(2)}$ is the nonlinear temporal susceptibility. Since the dispersion is relatively weak, we assumed in the right-hand side of the first equation in (1) that $v\approx v_g^{(\omega)}\approx c/n_\omega^{(0)}$, and in the right-hand side of the second equation that $v\approx v_g^{(2\omega)}\approx c/n_{2\omega}^{(0)}$. The first and second terms in the right-hand sides of Eqs. (1) describe the effect of the waveguide (transverse inhomogeneity) on the phase and group velocities of the harmonics, respectively. Since we consider quasimonochromatic signals, we do not include the terms $iq_{1,2}\frac{\partial\Phi_{1,2}}{\partial\tau}$ in (1). The latter can be done because we deal with pulses having about 100 oscillations under the envelope; thus, the coefficients of the terms corresponding to $iq_{1,2}\frac{\partial\Phi_{1,2}}{\partial\tau}$ are small in comparison with those corresponding to the terms $\omega q_{1,2}\Phi_{1,2}$.

Let the phase and group velocity matching conditions be satisfied, i.e., $k_2=2k_1$ ($n_\omega^{(0)}=n_{2\omega}^{(0)}=n$) and $v_g^{(\omega)}=v_g^{(2\omega)}=v_g$. Then the system (1) takes the form

$$\begin{aligned} i\frac{\partial\Phi_1}{\partial z}+\frac{\beta_\omega}{2}\frac{\partial^2\Phi_1}{\partial\tau^2}-\alpha_\omega\Phi_1^*\Phi_2 &= \omega q_1\Phi_1+\frac{c}{2n\omega}\frac{\partial^2\Phi_1}{\partial x^2}, \\ i\frac{\partial\Phi_2}{\partial z}+\frac{\beta_{2\omega}}{2}\frac{\partial^2\Phi_2}{\partial\tau^2}-\alpha_{2\omega}\Phi_1^2 &= 2\omega q_2\Phi_2+\frac{c}{4n\omega}\frac{\partial^2\Phi_2}{\partial x^2}. \end{aligned} \tag{3}$$

If the waveguide is focusing, then the functions $f_\omega(x)$ and $f_{2\omega}(x)$ decrease from the center to the periphery. In the opposite case, the waveguide is defocusing. In the case of an axially symmetric waveguide, the profiles of its functions are conveniently chosen, for example, in the parabolic form

$$f_\omega(r_\perp)=\varepsilon_w\frac{x^2}{a_\omega^2},\quad f_{2\omega}(r_\perp)=\varepsilon_w\frac{x^2}{a_{2\omega}^2}. \tag{4}$$

Here $a_{\omega,2\omega}$ are the waveguide widths, x is the distance from the center of the waveguide to a current point in the transversal direction, $\varepsilon_w=1$ for the defocusing waveguides at both frequencies, and $\varepsilon_w=-1$ for the focusing ones.

We proceed, seeking an approximate analytical solitonlike solution of the system (4) using the AL method [12,15–17]. First, we suppose in (4) that $f_\omega = f_{2\omega} = 0$ and the envelopes Φ_1 and Φ_2 are independent of x. In this case, under the condition

$$\beta_{2\omega} = 2\beta_\omega = 2\beta, \tag{5}$$

this system has a solution in the form of a one-dimensional (temporal) soliton [18]:

$$\Phi_1 = \pm\frac{3\beta}{2\sqrt{2\alpha_\omega\alpha_{2\omega}}\tau_p^2}\exp\left(i\frac{\beta}{2\tau_p^2}z\right)\mathrm{sech}^2\left(\frac{\tau}{2\tau_p}\right),$$
$$\Phi_2 = -\frac{3\beta}{4\alpha_\omega\tau_p^2}\exp\left(i\frac{\beta}{\tau_p^2}z\right)\mathrm{sech}^2\left(\frac{\tau}{2\tau_p}\right). \tag{6}$$

Here τ_p is a free parameter meaning the temporal duration of the soliton.

Let us briefly discuss a possibility of satisfying the equality (5) and the phase and group matching conditions as well. According to Sellmeier's formula [19], for the susceptibility $\chi_\omega = (\chi_0)/(1-\omega^2/\omega_0^2)$, where χ_0 is the static susceptibility of the medium, ω_0 is the characteristic frequency of the resonant absorption. In the low-frequency limit $\omega^2/\omega_0^2 \ll 1$ we have $\chi_\omega = \chi_0(1+\omega^2/\omega_0^2)$. Then the refractive index

$$n_\omega = \sqrt{1+4\pi\chi_\omega} = \sqrt{n_0^2 + \frac{4\pi\chi_0\omega^2}{\omega_0^2}} \approx n_0 + \frac{2\pi\chi_0\omega^2}{n_0\omega_0^2}, \tag{7}$$

where $n_0 = \sqrt{1+4\pi\chi_0}$. Relative smallness of the second term in (7) corresponds to a weak dispersion. Therefore, we can assume that $k \approx n_0\omega/c$ with an accurate approximation. Then $k_2 = k(2\omega) = 2k_1 = 2k(\omega)$. From here we also come to the equality $v_g^{(\omega)} \approx v_g^{(2\omega)} \approx c/n_0$. In addition, we find from (7) that $\beta_\omega = \frac{1}{c}\frac{\partial^2}{\partial\omega^2}(n_\omega\omega) = 12\pi\chi_0\omega/(cn_0\omega_0^2)$. Equality (5) automatically follows from the latter.

Thus, the phase and group matching conditions and the equality (5) can be approximately satisfied in the area of frequencies lying well below the frequencies of the resonant absorption. In this case $\beta_\omega > 0$. An analogous situation for $\beta_\omega < 0$ can be realized in the presence of spatial dispersion [20].

To take into account transverse perturbations due to the right-hand sides in (4), we use the solution (7). Now we assume that the soliton duration in (7) depends on the coordinates x and z. In addition, we suppose that the imaginary exponents are unknown coordinate-dependent functions. In this case, it is necessary to take into account modulation [21–23] and snake [23–26] instabilities that can affect one-dimensional solitons (7). Thus, we choose trial solutions in the form

$$\Phi_1 = \pm\frac{3\beta}{2\sqrt{2\alpha_\omega\alpha_{2\omega}}}\rho^{2/3}\exp\left(-i\left[\frac{n\omega}{c}\varphi + \eta(\tau+\xi)\right]\right)$$
$$\times\,\mathrm{sech}^2\left(\rho^{1/3}\frac{\tau+\xi}{2}\right),$$
$$\Phi_2 = -\frac{3\beta}{4\alpha_\omega}\rho^{2/3}\exp\left(-2i\left[\frac{n\omega}{c}\varphi + \eta(\tau+\xi)\right]\right)$$
$$\times\,\mathrm{sech}^2\left(\rho^{1/3}\frac{\tau+\xi}{2}\right), \tag{8}$$

where ρ, φ, η, and ξ are coordinate-dependent functions to be determined.

The functions ρ and φ describe the modulation instability. At the same time, the functions η and ξ describe the snake instability. In the one-dimensional case we have

$$\rho = \rho_0 = \frac{1}{\tau_p^3}, \quad \varphi = \varphi_0 = -\frac{c}{n\omega}\frac{\beta}{2\tau_p^2}z, \quad \eta = \xi = 0. \tag{9}$$

The parameter η has the meaning of small fluctuations in the carrier frequency of the fundamental component of the pulse. These fluctuations, in turn, due to dispersion give rise to fluctuations in the linear group velocity. As a result, the dynamic variable ξ becomes nonzero. Random curvatures of the wave fronts of the pulses are also inevitable. This leads to a local curvature of the phase and group stripes of solitons.

We note that the system (4) corresponds to the Lagrangian

$$L = L_1 + \frac{\alpha_\omega}{2\alpha_{2\omega}}L_2 + L_{\mathrm{int}},$$

where

$$L_1 = \frac{i}{2}\left(\Phi_1^*\frac{\partial\Phi_1}{\partial z} - \Phi_1\frac{\partial\Phi_1^*}{\partial z}\right) - \omega q_1|\Phi_1|^2$$
$$-\frac{\beta_\omega}{2}\left|\frac{\partial\Phi_1}{\partial\tau}\right|^2 + \frac{c}{2n\omega}\left|\frac{\partial\Phi_1}{\partial x}\right|^2,$$
$$L_2 = \frac{i}{2}\left(\Phi_2^*\frac{\partial\Phi_2}{\partial z} - \Phi_2\frac{\partial\Phi_2^*}{\partial z}\right) - 2\omega q_2|\Phi_2|^2$$
$$-\frac{\beta_{2\omega}}{2}\left|\frac{\partial\Phi_2}{\partial\tau}\right|^2 + \frac{c}{4n\omega}\left|\frac{\partial\Phi_2}{\partial x}\right|^2,$$
$$L_{\mathrm{int}} = -\alpha_{2\omega}\left(\Phi_1^{*2}\Phi_2 + \Phi_1^2\Phi_2^*\right).$$

According to the AL method, we substitute the trial solutions (9) in these expressions for the Lagrangian and integrate the outcome expression with respect to the local time τ. Taking into account the equality (5), we obtain as a result

$$\int_{-\infty}^{+\infty} L\,d\tau = \frac{9n\omega}{2c}\frac{\beta^2}{\alpha_\omega\alpha_{2\omega}}\Lambda, \tag{10}$$

where the averaged Lagrangian Λ looks like

$$\Lambda = \rho\frac{\partial\varphi}{\partial z} + \frac{\rho}{2}\left(\frac{\partial\varphi}{\partial x}\right)^2 + \frac{3}{10}\frac{c}{n\omega}\beta\rho^{5/3} - \frac{c}{n}q\rho$$
$$+\frac{g^2}{2}\left(\frac{c}{n\omega}\right)^2\frac{1}{\rho}\left(\frac{\partial\rho}{\partial x}\right)^2 - \frac{c}{n\omega}\rho\eta\frac{\partial\xi}{\partial z}$$
$$-\frac{c}{n\omega}\beta\rho\eta^2 + \frac{1}{2}\left(\frac{c}{n\omega}\right)^2\left(\frac{3}{20}\rho^{5/3} + \rho\eta^2\right)\left(\frac{\partial\xi}{\partial x}\right)^2$$
$$-\frac{c}{n\omega}\rho\eta\frac{\partial\varphi}{\partial x}\frac{\partial\xi}{\partial x} + \frac{b^2}{2}\left(\frac{c}{n\omega}\right)^2\rho^{1/3}\left(\frac{\partial\eta}{\partial x}\right)^2, \tag{11}$$

where $g^2 = \frac{1}{6}(\frac{\pi^2}{30}+1)(\frac{c}{n\omega})^2$, $b^2 = 2(\frac{\pi^2}{6}-1)(\frac{c}{n\omega})^2$. Taking into account both (2) and matching conditions ($n_\omega^{(0)} = n_{2\omega}^{(0)} = n$, $\chi_\omega^{(0)} = \chi_{2\omega}^{(0)} = \chi$), we rewrite the expression for q in (11) in the form

$$q = \frac{2\pi}{cn}\chi f = \frac{n^2-1}{2cn}f, \quad f = \frac{2f_\omega + f_{2\omega}}{3}. \tag{12}$$

Using the Euler-Lagrange equations

$$\begin{aligned}\frac{\partial}{\partial z}\frac{\partial\Lambda}{\partial(\partial\varphi/\partial z)}+\frac{\partial}{\partial x}\frac{\partial\Lambda}{\partial(\partial\varphi/\partial x)}=0,\\ \frac{\partial\Lambda}{\partial\rho}-\frac{\partial}{\partial x}\frac{\partial\Lambda}{\partial(\partial\rho/\partial x)}=0,\\ \frac{\partial}{\partial z}\frac{\partial\Lambda}{\partial(\partial\xi/\partial z)}+\frac{\partial}{\partial x}\frac{\partial\Lambda}{\partial(\partial\xi/\partial x)}=0,\\ \frac{\partial\Lambda}{\partial\eta}-\frac{\partial}{\partial x}\frac{\partial\Lambda}{\partial(\partial\eta/\partial x)}=0,\end{aligned} \tag{13}$$

after simple mathematical transformations we come to the set of equations

$$\frac{\partial\rho}{\partial z}+\frac{\partial}{\partial x}\left[\rho\frac{\partial}{\partial x}\left(\varphi+\frac{c}{n\omega}\eta\xi\right)\right]=0, \tag{14}$$

$$\begin{aligned}&\frac{\partial\varphi}{\partial z}+\frac{1}{2}\left(\frac{\partial\varphi}{\partial x}\right)^2+\frac{c}{2n\omega}\beta\rho^{2/3}-\frac{c}{n}q(x)\\ &=\frac{2g^2}{\sqrt{\rho}}\frac{\partial^2\sqrt{\rho}}{\partial x^2}-\frac{c}{n\omega}\beta\eta^2-b^2\frac{\eta}{\rho}\frac{\partial}{\partial x}\left(\rho^{1/3}\frac{\partial\eta}{\partial x}\right)\\ &\quad+\frac{1}{2}\left(\frac{c}{n\omega}\right)^2\left(\eta^2-\frac{\rho^{2/3}}{4}\right)\left(\frac{\partial\xi}{\partial x}\right)^2\\ &\quad-\frac{2}{9\rho^{2/3}}\left(\frac{c}{n\omega}\right)^2\left(\frac{\partial\eta}{\partial x}\right)^2,\end{aligned} \tag{15}$$

$$\frac{\partial\eta}{\partial z}+\frac{\partial\eta}{\partial x}\frac{\partial}{\partial x}\left(\varphi+\frac{c}{n\omega}\eta\xi\right)+\frac{3}{20}\frac{c}{n\omega}\frac{1}{\rho}\frac{\partial}{\partial x}\left(\rho^{5/3}\frac{\partial\xi}{\partial x}\right), \tag{16}$$

$$\begin{aligned}\frac{\partial\xi}{\partial z}&=2\beta\eta+b^2\frac{n\omega}{c}\frac{1}{\rho}\frac{\partial}{\partial x}\left(\rho^{1/3}\frac{\partial\eta}{\partial x}\right)\\ &\quad-\frac{\partial\varphi}{\partial x}\frac{\partial\xi}{\partial x}-\frac{c}{n\omega}\eta\left(\frac{\partial\xi}{\partial x}\right)^2.\end{aligned} \tag{17}$$

The parameters of the one-dimensional (1D) soliton are independent of the transverse coordinate x. From (14) and (16) in this case we have $\frac{\partial\rho}{\partial z}=\frac{\partial\eta}{\partial z}=0$. Assuming in accordance with this $\rho=\tau_p^{-3}=\text{const}$, $\eta=0$ [see (9)], from (17) and (15) under condition $q(x)=0$ we have $\frac{\partial\xi}{\partial z}=0$, $\frac{\partial\varphi}{\partial z}=-\frac{c}{n\omega}\frac{\beta}{2\tau_p^2}$. These conditions strictly correspond to the equalities (9). Thus, in the 1D case the trial solutions (9) coincide exactly with the solutions (7). This circumstance is an important argument in favor of the AL method.

As can be seen from the system (14)–(17), the dynamic variables describing modulation and snake instabilities are connected with each other. To simplify the procedure for further studies, we consider the small perturbations of the parameters of a one-dimensional soliton, assuming

$$\rho=\frac{1}{\tau_p^3}+\rho_1,\quad \varphi=-\frac{c}{n\omega}\frac{\beta}{2\tau_p^2}z+\varphi_1. \tag{18}$$

By means of a linearization of the system (14)–(17) with respect to the variables ρ_1, φ_1, η, and ξ we obtain

$$\frac{\partial\rho_1}{\partial z}=-\frac{1}{\tau_p^3}\frac{\partial^2\varphi_1}{\partial x^2}, \tag{19}$$

$$\frac{\partial\varphi_1}{\partial z}=-\frac{c\beta\tau_p}{3n\omega}\rho_1+\frac{c}{n}q(x)+g^2\tau_p^3\frac{\partial^2\rho_1}{\partial x^2}, \tag{20}$$

$$\frac{\partial\eta}{\partial z}=-\frac{3}{20\tau_p^2}\frac{c}{n\omega}\frac{\partial^2\xi}{\partial x^2}, \tag{21}$$

$$\frac{\partial\xi}{\partial z}=2\beta\eta+b^2\frac{n\omega}{c}\tau_p^2\frac{\partial^2\eta}{\partial x^2}. \tag{22}$$

Thus, in the linear approximation, the dynamic parameters corresponding to the modulation and snake instabilities are independent of each other. Note that a similar situation occurs in the case of these instabilities for a soliton of the nonlinear Schrödinger equation propagating in a gradient waveguide [27].

Excluding the variable φ_1 from the system (19), (20), we obtain

$$\frac{\partial^2\rho_1}{\partial z^2}=\frac{c\beta}{3n\omega\tau_p^2}\frac{\partial^2\rho_1}{\partial x^2}-\frac{c}{n\tau_p^3}\frac{d^2q}{dx^2}-g^2\frac{\partial^4\rho_1}{\partial x^4}. \tag{23}$$

In the case of a parabolic profile of the linear refractive index determined by the expressions (2) and (4), we have $d^2q/dx^2=\text{const}$. Then Eq. (23) can be written as

$$\frac{\partial^2\tilde{\rho}}{\partial z^2}=\varepsilon_d\frac{2}{3l_d}\frac{c}{n\omega}\frac{\partial^2\tilde{\rho}}{\partial x^2}-g^2\frac{\partial^4\tilde{\rho}}{\partial x^4}, \tag{24}$$

where $l_d=\frac{2\tau_p^2}{|\beta|}$ is the dispersion length, $\tilde{\rho}=\rho_1-\frac{3}{2}\frac{\varepsilon_d}{\tau_p^3}\omega l_d q(x)$; $\varepsilon_d=\text{sgn}\beta$, i.e., if GVD is normal, $\varepsilon_d=+1$, otherwise for anomalous GVD $\varepsilon_d=-1$.

From (19) and (20) it is easy to get Eq. (24) for φ_1.

From (21) and (22) we find

$$\frac{\partial^2\eta}{\partial z^2}=-\varepsilon_d\frac{3}{5l_d}\frac{c}{n\omega}\frac{\partial^2\eta}{\partial x^2}-\frac{3}{20}b^2\frac{\partial^4\eta}{\partial x^4}. \tag{25}$$

The dynamic parameter ξ obeys the same equation.

Assuming in (24) and (25) that $\tilde{\rho}\sim e^{\Gamma_m z}\cos kx$, $\eta\sim e^{\Gamma_s z}\cos kx$, we obtain the expressions for the increments of modulation Γ_m and snake Γ_s instabilities:

$$\Gamma_m^2=-\frac{2}{3}\varepsilon_d\frac{c}{n\omega l_d}k^2-g^2k^4, \tag{26}$$

$$\Gamma_s^2=\frac{3}{5}\varepsilon_d\frac{c}{n\omega l_d}k^2-\frac{3}{20}b^2k^4. \tag{27}$$

Let GVD be anomalous, i.e., $\varepsilon_d=-1$. Then, as can be seen from (26), the modulation instability develops under condition $k<k_m=1.73\sqrt{\frac{n\omega}{cl_d}}$. In this case a snake instability does not occur.

If GVD is normal ($\varepsilon_d=+1$), the situation is opposite: under the condition $k<k_s=1.76\sqrt{\frac{n\omega}{cl_d}}$ [see (27)], the snake instability develops, and a modulation instability does not occur.

These conclusions qualitatively coincide with the results obtained previously for solitons in media with Kerr nonlinearity [22].

Under the condition $k>k_s,k_m$ both instabilities are suppressed at both normal and anomalous dispersion. Putting $k\sim 1/R_0$, where R_0 is a characteristic transverse size (aperture) of the soliton, we find that both instabilities can be suppressed under the condition $l_D<l_d$. Here $l_D=\frac{n\omega}{c}R_0^2$ is the diffraction length. In this case, it can be assumed that the localization of

the pulse in the transverse directions occurs mainly due to the focusing waveguide effect.

It was shown in [27] that a gradient focusing waveguide suppresses snake instability in a medium with Kerr nonlinearity. Formulas (26) and (27), up to coefficients, coincide with similar formulas obtained in the case of the Kerr nonlinearity [22,24]. Therefore, we assume in advance that the snake instability in our case is also suppressed by the focusing waveguide effect under normal GVD. Below we will consider only the modulation instability, which, together with a focusing waveguide under conditions of anomalous GVD, creates the localization effect of pulses of the fundamental frequency and second harmonic. Under this assumption, in the case of normal GVD, the transverse localization effect is created solely due to the waveguide effect. We emphasize in advance that this assumption is confirmed by numerical experiments, the results of which are presented in Sec. IV. We note, however, that with this approach it is impossible to completely and strictly consider the case of normal GVD and a defocusing waveguide. However, as will be shown below, in this case, stable light bullets cannot be formed. For this reason, we will not study this case in detail.

Summarizing the above, we put in (14)–(17) $\eta = \xi = 0$. Then Eqs. (16) and (17) turn into identities $0 = 0$, and Eqs. (14) and (15) take the form

$$\frac{\partial \rho}{\partial z} + \frac{\partial}{\partial x}\left(\rho \frac{\partial \varphi}{\partial x}\right) = 0, \tag{28}$$

$$\frac{\partial \varphi}{\partial z} + \frac{1}{2}\left(\frac{\partial \varphi}{\partial x}\right)^2 + \frac{c}{2n\omega}\beta\rho^{2/3} - \frac{c}{n}q(x) = \frac{2g^2}{\sqrt{\rho}}\frac{\partial^2\sqrt{\rho}}{\partial x^2}. \tag{29}$$

Moreover, we must put $\eta = \xi = 0$ in expressions (9). Then we will have trial solutions in the form of an *ansatz* used to take into account the influence of transverse perturbations on the plane solitons [22].

The system (28), (29) is analogous to the system of equations for a quantum Bose liquid in an external field [28]. Equation (28) is the continuity equation, and Eq. (29) is the quantum integral of Cauchy. The third term in the left-hand side of (29) corresponds to the interaction between particles of an imaginary liquid, which forms internal pressure. In the problem we are solving this term corresponds to nonlinearity and GVD. The fourth term (taking into account the waveguide) describes the effect of an external field on the flow of a fluid. The right-hand side is often called quantum pressure. It takes into account the wave properties of particles of an imaginary quantum liquid. In our case the right-hand side in (29) corresponds to the influence of diffraction on the propagation of the pulses of both harmonics. If we put in (29) $g = 0$, we take into consideration transverse perturbations in the approximation of geometric optics. In this case, transversal perturbations are accounted for by the second terms in the left-hand sides of Eqs. (28) and (29), which coincide at $q = 0$ with the equations of motion of the classical ideal fluid.

Analogy between the dynamics of an optical soliton in a waveguide and the flow of a quantum Bose liquid in an external field can be used to apply the Madelung transformation [1]

$$Q = \sqrt{\rho}\exp\left(i\frac{\varphi}{2g}\right).$$

It is easy to see that the system (28), (29) is equivalent to the following equation for a complex function Q:

$$i\frac{\partial Q}{\partial z} = -g\frac{\partial^2 Q}{\partial x^2} + \frac{c}{2gn}\left(\frac{\beta}{2\omega}|Q|^{4/3} - q(x)\right)Q. \tag{30}$$

This equation is analogous to the Gross-Pitaevskii (GP) equation [29], which describes the dynamics of the Bose-Einstein condensate in an external field. Equation (30) differs from GP in the nonlinear term. In (30) this term has the form $\sim|Q|^{4/3}Q$, and in the GP equation the nonlinear term looks like $\sim|Q|^2Q$. Therefore, we call Eq. (30) the modified Gross-Pitaevskii equation (MGP).

III. APPROXIMATE ANALYTICAL SOLUTIONS AND THEIR STABILITY

In the planar case, for $q = 0$ and $\beta < 0$ (in the absence of a waveguide and at anomalous GVD) the system (28), (29) [or Eq. (30)] has an exact localized solution [12]. Frequency ω is by definition a positive value. On the other hand, if we formally put in (30) $\beta = 0$, then we come to the linear quantum-mechanical Schrödinger equation. There are many kinds of functions $q(x)$ for which this equation has exact solutions. In general, when $\beta \neq 0$ and $q(x) \neq 0$, there are probably no exact analytical solutions. Therefore, we restrict our consideration to the search for an approximate solution corresponding to a localized spatial-temporal soliton.

First we make the analysis in the framework of geometric optics. Equation (28) has an exact self-similar solution of the form [30]

$$\rho = \frac{1}{\tau_p^3}\frac{R_0}{R}G\left(\frac{x}{R}\right), \quad \varphi = \sigma(z) + \frac{x^2}{2R}\frac{dR}{dz}, \tag{31}$$

where R and σ are still unknown functions of z, and G is also an unknown dimensionless function of its argument x/R. The second term in the right-hand side of (31) describes the dynamic curvature of the wave fronts of the pulse as it propagates in the medium.

Let us consider the values of the transverse coordinate that satisfy the condition

$$\left(\frac{x}{a_{\omega,2\omega}}\right)^2 \ll 1. \tag{32}$$

From (4) and (12) we have

$$q = \varepsilon_w\frac{n^2-1}{2cn}\frac{x^2}{a^2}, \tag{33}$$

where $a^2 = 3(2a_\omega^{-2} + a_{2\omega}^{-2})^{-1}$.

To find the functions R, σ, and G let us substitute (31) into (29), taking into account (33), using the approximation of geometric optics ($g = 0$). Then

$$\frac{d\sigma}{dz} + \frac{x^2}{2R}\frac{d^2R}{dz^2} + \varepsilon_d\frac{c}{n\omega l_d}\frac{R_0^{2/3}}{R^{2/3}}G^{2/3} - \varepsilon_w\frac{n^2-1}{2n^2}\frac{x^2}{a^2} = 0. \tag{34}$$

We should choose the function $G(x/R)$, guided by two considerations: (a) it is necessary to obtain an exact solution; (b) the variable ρ must be localized along the x axis. Both

conditions are satisfied by the expression

$$G^{2/3} = 1 - \frac{x^2}{4R^2}, \quad |x| < 2R. \tag{35}$$

From (35), (31), and (9) it is clear that the parameter R has the meaning of the transverse aperture of the soliton.

Then, equating to zero the expressions at x^0 and x^2 in the left-hand side of (34), we come to the equations

$$\frac{d\sigma}{dz} = -\varepsilon_d \frac{c}{n\omega l_d}\beta\frac{R_0^{2/3}}{R^{2/3}}, \tag{36}$$

$$\frac{d^2R}{dz^2} = \varepsilon_d \frac{c}{2n\omega l_d}\frac{R_0^{2/3}}{R^{5/3}} + \varepsilon_w \frac{n^2-1}{n^2a^2}R. \tag{37}$$

Here $\tau_p = 1/\rho_0^{1/3}$ is the pulse duration on its axis [at $x = 0$; see (31), (32) and (34), (35)[.

The value $d\sigma/dz$ is proportional to the nonlinear addition to the refractive index on the waveguide axis [see (31), (9)]. The first and second terms in the right-hand side of (37) describe nonlinear and linear (waveguide) refraction, respectively.

Expressions (31) and (35) represent the exact solution of the system (28), (29) at $g = 0$. In this case, the dependence $R(z)$ can be found as a result of integrating Eq. (37) in quadratures.

Now let us approximately take into account the influence of diffraction ($g \neq 0$). It is clear that diffraction leads to the blurring of sharp boundaries of the light bullet, described by the expression (35). In accordance with this, starting from (35), we set [12]

$$G^{2/3} = \mathrm{sech}^2\left(\frac{x}{2R}\right). \tag{38}$$

In this case, the right-hand side of (34) takes the form

$$\frac{2g^2}{\sqrt{\rho}}\frac{\partial^2\sqrt{\rho}}{\partial x^2} = \frac{2g^2}{\sqrt{F}}\frac{\partial^2\sqrt{F}}{\partial x^2} = \frac{9g^2}{8R^2}\left[1 - \frac{5}{3}\mathrm{sech}^2\left(\frac{x}{2R}\right)\right].$$

Assuming the near-axis approximation $x^2/R^2 \ll 1$ [31], we write $\mathrm{sech}^2(\frac{x}{2R}) \approx 1 - \frac{x^2}{4R^2}$. Then, instead of (36) and (37), we have

$$\frac{d\sigma}{dz} = -\varepsilon_d \frac{c}{n\omega l_d}\frac{R_0^{2/3}}{R^{2/3}} - \frac{3g^2}{4R^2}, \tag{39}$$

$$\frac{d^2R}{dz^2} = -\frac{\partial U}{\partial R}, \tag{40}$$

where the "potential energy"

$$U = \varepsilon_d \frac{3c}{4n\omega l_d}\frac{R_0^{2/3}}{R^{2/3}} - \varepsilon_w \frac{n^2-1}{2n^2a^2}R^2 + \frac{15g^2}{32R^2}. \tag{41}$$

The last terms in the right-hand sides of (39) and (41) describe the effect of diffraction. Equation (40) is formally similar to the equation of motion of a Newtonian particle of unit mass. The roles of the coordinate and time are played by the pulse aperture R and z coordinate, respectively. The first integral of this equation has the form

$$\frac{1}{2}\left(\frac{dR}{dz}\right)^2 + U(R) = \mathrm{const}. \tag{42}$$

The case $R = R_0 = \mathrm{const}$ corresponds to the stationary propagation of a spatial-temporal soliton with plane wave fronts. Amplitudes of its both components decrease from the center to the peripheral regions as $\sim\mathrm{sech}^2(\frac{x}{2R_0})$, and the duration increases according to the law $\sim\mathrm{sech}(\frac{x}{2R_0})$ [see (38), (31), and (9)].

The stability conditions for such a stationary solution have the form

$$\left(\frac{\partial U}{\partial R}\right)_{R=R_0} = 0, \quad \left(\frac{\partial^2 U}{\partial R^2}\right)_{R=R_0} > 0.$$

These conditions correspond to the minimum of "potential energy" for an imaginary particle of unit mass [see (40)]. Therefore, these equilibrium positions are stable.

From this and (41), taking into account $\frac{3}{4}(\frac{\pi^2}{30} + 1) = 0.997 \approx 1$, we find

$$\varepsilon_d + \varepsilon_w\frac{\mu}{3} + \frac{5}{12}\frac{l_d}{l_D} = 0, \tag{43}$$

$$\varepsilon_w\mu + \varepsilon_d < 0. \tag{44}$$

Here we determine

$$\mu = \frac{6l_d l_D(n^2-1)}{a^2n^2} \tag{45}$$

and the dispersion l_d and diffraction l_D lengths

$$l_d = \frac{2\tau_p^2}{|\beta|}, \quad l_D = \frac{n\omega}{c}R_0^2.$$

$\varepsilon_d = \mathrm{sgn}\,\beta$, i.e., if GVD is normal, $\varepsilon_d = +1$, otherwise for anomalous GVD $\varepsilon_d = -1$.

So, for the formation of a two-color light bullet, simultaneous fulfillment of the conditions (43) and (44) is necessary.

For a homogeneous medium we have $a \to \infty$. Then we find from (27) $\varepsilon_d = -1$. Thus, to form a stable light bullet in a homogeneous medium, GVD must be anomalous [12]. In this case, equality (43) can be rewritten as $l_D = 5l_d/12 \approx 0.42l_D$. This also coincides with the result obtained earlier in [12].

It follows from (43) that, under condition $\varepsilon_d = \varepsilon_w = +1$ (normal GVD, defocusing waveguide), it is impossible to form a light bullet. In this case, the snake instability considered above in the linear approximation is added to the defocusing instability created by the waveguide. The results of numerical experiments confirm the conclusion that it is impossible to form a light bullet in this case. In the remaining three cases, bullet formation is possible. Let us consider these cases in more detail.

a. Anomalous GVD, defocusing waveguide ($\varepsilon_d = -1$, $\varepsilon_w = +1$). In this case from (43) and (44) we find

$$\frac{\mu}{3} = 1 - \frac{5}{12}\frac{l_d}{l_D}, \tag{46}$$

$$\mu < 1. \tag{47}$$

Successively excluding the parameters a, l_d, and l_D from the conditions (46) and (47), taking into account (45), we arrive

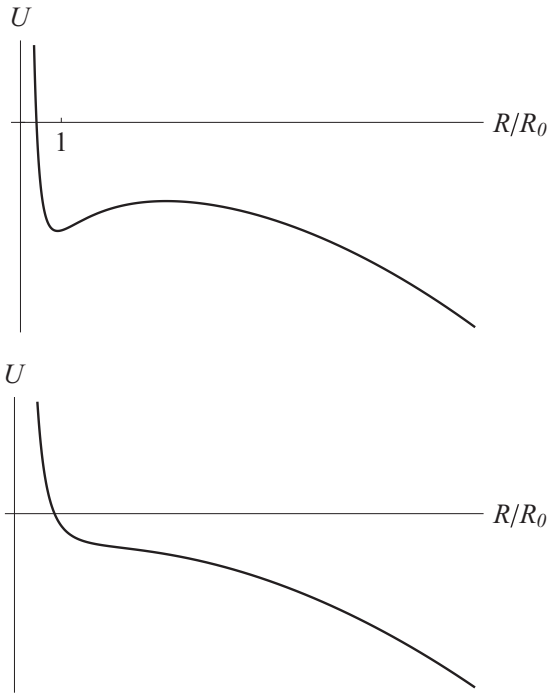

FIG. 1. Schematic representation of the dependence of "potential energy" U on the dimensionless pulse aperture R/R_0 of a pulse under conditions (48) (top) and under violation of these conditions (bottom); anomalous GVD and defocusing waveguide: $e_d = -1$, $e_w = +1$.

at the inequalities

$$1.60 < \frac{l_d}{l_D} < 2.40, \quad \frac{l_D}{a} < 0.32\frac{n}{\sqrt{n^2-1}}, \quad \frac{l_d}{a} < 0.55\frac{n}{\sqrt{n^2-1}}. \tag{48}$$

Note that the right-hand side of the first of the inequalities (48) automatically follows from (46). We write it in the form of a double inequality in order to emphasize that the light bullet is formed in a narrow interval of the ratio l_d/l_D. It is easy to see from (42) that if the conditions (48) are violated, the pulse is defocused.

This case is schematically shown in Fig. 1 in the form of dependences of "potential energy" U on R, when conditions (48) are satisfied and if they are violated. Note that in a defocusing waveguide with a focusing Kerr nonlinearity, the formation of stable spatiotemporal solitons is impossible. In this case, the waveguide should be focusing [29]. Therefore, the conditions (48), under which the formation of light bullets is possible, are applicable only to quadratically nonlinear media.

b. Anomalous GVD, focusing waveguide ($\varepsilon_d = -1$, $\varepsilon_w = -1$). In this case we find

$$\frac{\mu}{3} = \frac{5}{12}\frac{l_d}{l_D} - 1. \tag{49}$$

Provided that this equality holds, the condition (44) is satisfied automatically. Therefore, additional restrictions, along with (49), are not required.

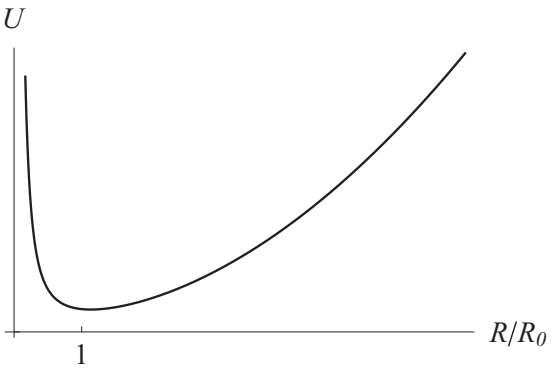

FIG. 2. Schematic representation of the dependence of "potential energy" U on the dimensionless pulse aperture R/R_0 in cases of anomalous ($e_d = -1$) or normal ($e_d = +1$) GVD and of focusing waveguide ($e_w = -1$). In both cases the function $U(R/R_0)$ has a clearly defined minimum at $R/R_0 = 1$, which indicates the stability of the spatiotemporal soliton.

In the case of the Kerr nonlinearity condition under consideration, the optical pulse can develop a collapse ($R \to 0$, $\rho \to \infty$) in a finite time if the pulse power exceeds a certain threshold value [32,33]. With quadratic nonlinearity collapse does not occur. For the case of a homogeneous quadratically nonlinear medium this was shown in [12,34]. As can be seen from Fig. 2, the development of collapse is also impossible in the focusing waveguide, because $U \to \infty$ at $R \to 0$.

c. Normal GVD, focusing waveguide ($\varepsilon_d = +1$, $\varepsilon_w = -1$). In this case we have

$$\frac{\mu}{3} = 1 + \frac{5}{12}\frac{l_d}{l_D}. \tag{50}$$

Inequality (44) $\mu > 1$ is satisfied automatically (see Fig. 2), because from (50) we have $\mu > 3$. Assuming in (50) that $a \to \infty$ ($\mu \to 0$), we conclude that it is impossible to form a light bullet at normal GVD in a homogeneous medium. This is a well-known result supported by theory and experiments [1].

Formulas (46)–(50) refer to the steady-state propagation mode, when the soliton aperture and its duration are constants. Then we can write down the following solution in an explicit form:

$$\Phi_1 = \pm\frac{3\beta}{2\sqrt{2\alpha_\omega\alpha_{2\omega}}\tau_p^2}\exp\left(i\frac{\beta z}{2\tau_p^2}\right) \times \operatorname{sech}^2\left(\frac{x}{2R_0}\right)\operatorname{sech}^2\left[\frac{\tau}{2\tau_p}\operatorname{sech}\left(\frac{x}{2R_0}\right)\right],$$
$$\Phi_2 = -\frac{3\beta}{4\alpha_\omega\tau_p^2}\exp\left(i\frac{\beta z}{\tau_p^2}\right) \times \operatorname{sech}^2\left(\frac{x}{2R_0}\right)\operatorname{sech}^2\left[\frac{\tau}{2\tau_p}\operatorname{sech}\left(\frac{x}{2R_0}\right)\right]. \tag{51}$$

It is important to note that, according to the expression (33), an effective waveguide is formed at both harmonics. In this case, situations are possible where the waveguide exists only for one harmonic. In these cases $1/a_\omega = 0$ or $1/a_{2\omega} = 0$, but $1/a \neq 0$. Let, for example, $1/a_\omega = 0$, $1/a_{2\omega} \neq 0$, $\varepsilon_w = -1$. Then the input pulse of the fundamental harmonic

generates a second harmonic pulse in the medium. In turn, the second harmonic pulse can capture the fundamental harmonic pulse into the waveguide.

In this section, the expressions (9) are chosen as trial functions, i.e., it is assumed that pulses of both harmonics are formed in the medium. However, the greatest interest is a study of the formation of light bullets in the process of SHG. This corresponds to the situation when there is no second harmonic at the input to the medium. Moreover, under real conditions it is very difficult to achieve simultaneous fulfillment of phase and group matching conditions [see (5)].

It is useful to specify the period of spatial oscillations of the aperture. Conditions (43) and (44) correspond to the presence of a minimum of "potential energy" $U(R)$ at $R = R_0$. For small deviations from this minimum, the oscillatory mode of the aperture $R(z)$ should be realized near the equilibrium value R_0. We put in (40) $R = R_0 + \xi$, where $|\xi| \ll R_0$. After linearization with respect to ξ, we obtain

$$\frac{d^2\xi}{dz^2} = -\left(\frac{2\pi}{T}\right)^2 \xi,$$

where T is the period of small spatial oscillations of the aperture, determined by the relation

$$T = \frac{T_0}{\sqrt{-\varepsilon_d - \varepsilon_w \mu}}; \tag{52}$$

$T_0 = 2\pi\sqrt{3l_d l_D/2} \approx 7.70\sqrt{l_d l_D}$ is the period of spatial oscillations in the absence of waveguide at $\varepsilon_d = -1$. Three cases mentioned above correspond to the expressions for periods:

$$T_a = \frac{T_0}{\sqrt{1-\mu}}, \quad T_b = \frac{T_0}{\sqrt{1+\mu}}, \quad T_c = \frac{T_0}{\sqrt{\mu-1}}. \tag{53}$$

We emphasize once again that the conditions (43) and (44) are related to the steady-state light bullet (51). The answer to the question of how to generate such a bullet can be given by means of numerical simulation.

The generation mode in the absence of at least one of the matching conditions (phase or group) can be investigated, perhaps, only with the help of numerical simulations on the basis of Eqs. (1) as well. This is discussed in detail in the next section.

IV. RESULTS OF NUMERICAL SIMULATION IN PLANAR WAVEGUIDE AND DISCUSSION

In this section we discuss the outcome of a direct numerical simulation of the system (1) which we performed to confirm our analytical results presented in the previous section and to widen the scope of our study, including the effects neglected in the analytical approach and a possibility of light bullet formation in a waveguide at SHG.

We still consider a planar waveguide and use dimensionless parameters related to the physical parameters in the following way: $\Phi_{1,2} = A_{1,2}A_{in}$, $z = \bar{z}l_{nl}$, $x = \bar{x}R_{in}$, $\tau = \bar{\tau}\tau_{in}$, $\Delta\bar{k} = \Delta k l_{nl}$, $\Delta k = 2k_1 - k_2$ is the phase detuning, $l_{nl} = (\alpha_\omega A_{in})^{-1}$ is the nonlinear length, and $a_{\omega,2\omega} = R_{in}\bar{a}_{\omega,2\omega}$. Here A_{in} is the input peak amplitude of the fundamental harmonic and R_{in} and τ_{in} are initial pulse spatial and temporal widths, respectively. We introduce also the following propagation and waveguide characteristics: $D_{q1} = 2\pi\omega l_{nl}\chi_\omega^{(0)}\varepsilon_w/(cn_\omega^{(0)}\bar{a}_\omega^2)$, $D_{q2} = 4\pi\omega l_{nl}\chi_{2\omega}^{(0)}\varepsilon_w/(cn_{2\omega}^{(0)}\bar{a}_{2\omega}^2)$, $D_{\tau 1} = \beta_\omega l_{nl}/(2\tau_{in}^2)$, $D_{\tau 2} = \beta_{2\omega} l_{nl}/(2\tau_{in}^2)$, $D_{x1}=cl_{nl}/(2\omega n_\omega^{(0)}R_{in}^2)$, $D_{x2}=cl_{nl}/(4\omega n_{2\omega}^{(0)}R_{in}^2)$; $\gamma = \alpha_{2\omega}/\alpha_\omega$, a_ω, and $a_{2\omega}$ are the characteristic lengths of waveguide transversal inhomogeneity. Spatial and temporal widths of an arising soliton, which generally are different from those of the initial pulse, we normalize as $R_0 = \bar{R}_0 R_{in}$, $\tau_p = \bar{\tau}_0\tau_{in}$. Then, we suppose the group matching conditions are satisfied, $v_g^{(\omega)} = v_g^{(2\omega)} = v_g$. Finally, we get the following system of the dimensionless equations, which we use as a base for our numerical simulation:

$$\begin{aligned} i\frac{\partial A_1}{\partial\bar{z}} &= D_{q1}\bar{x}^2 A_1 - D_{\tau 1}\frac{\partial^2 A_1}{\partial\bar{\tau}^2} + A_1^* A_2 e^{i\Delta\bar{k}\bar{z}} + D_{x1}\frac{\partial^2 A_1}{\partial\bar{x}^2}, \\ i\frac{\partial A_2}{\partial\bar{z}} &= D_{q2}\bar{x}^2 A_2 - D_{\tau 2}\frac{\partial^2 A_2}{\partial\bar{\tau}^2} + \gamma A_1^2 e^{-i\Delta\bar{k}\bar{z}} + D_{x2}\frac{\partial^2 A_2}{\partial\bar{x}^2}. \end{aligned} \tag{54}$$

The system (54) possesses the motion integrals [14]

$$I_1 = \int_{-\infty}^{\infty} d\bar{x}\int_{-\infty}^{\infty}(\gamma|A_1|^2 + |A_2|^2)d\bar{\tau}, \tag{55}$$

$$\begin{aligned} I_3 = \int_{-\infty}^{\infty} d\bar{x}\int_{-\infty}^{\infty} d\bar{\tau}\Bigg\{ & -2\left|A_1^2 A_2\right|\cos(2\varphi_1 - \varphi_2) \\ & + \frac{\Delta\bar{k}}{\gamma}|A_2|^2 + 2D_{x1}\left|\frac{\partial A_1}{\partial\bar{x}}\right|^2 + D_{x2}\gamma^{-1}\left|\frac{\partial A_2}{\partial\bar{x}}\right|^2 \\ & - 2D_{\tau 1}\left|\frac{\partial A_1}{\partial\bar{\tau}}\right|^2 - D_{\tau 2}\gamma^{-1}\left|\frac{\partial A_2}{\partial\bar{\tau}}\right|^2 \\ & - 2D_{q1}\bar{x}^2|A_1|^2 - D_{q2}\bar{x}^2\gamma^{-1}|A_2|^2\Bigg\}. \end{aligned} \tag{56}$$

In (56) $\varphi_{1,2}$ are the wave phases.

The principal interest in our numerical experiment is to check whether our approximate solutions (51) and criteria (46)–(50) demonstrate a sufficient coincidence with the results revealed in direct numerical simulation of the system (54). Moreover, we go beyond the framework of the theoretical analysis and show a possibility of light bullet capture and stable propagation at SHG and at a certain phase mismatch as well. In computations we launch the initial pulse at both frequencies in the form corresponding to (51),

$$\begin{aligned} A_1(\bar{z}=0) &= E\,\mathrm{sech}^2\left(\frac{\bar{x}}{2}\right)\mathrm{sech}^2\left[\frac{\bar{\tau}}{2}\,\mathrm{sech}\left(\frac{\bar{x}}{2}\right)\right], \\ A_2(\bar{z}=0) &= \pm\frac{E}{2}\,\mathrm{sech}^2\left(\frac{\bar{x}}{2}\right)\mathrm{sech}^2\left[\frac{\bar{\tau}}{2}\,\mathrm{sech}\left(\frac{\bar{x}}{2}\right)\right], \end{aligned} \tag{57}$$

or at the fundamental frequency only,

$$\begin{aligned} A_1(\bar{z}=0) &= E\,\mathrm{sech}^2\left(\frac{\bar{x}}{2}\right)\mathrm{sech}^2\left[\frac{\bar{\tau}}{2}\,\mathrm{sech}\left(\frac{\bar{x}}{2}\right)\right], \\ A_2(\bar{z}=0) &= 0. \end{aligned} \tag{58}$$

Then, taking into account (51) and the way of normalization, we put in (57) $E = 3D_{\tau 1}$. In the process of SHG there is a partial dissipation of the energy of the fundamental harmonic, therefore, in our calculations we take $E \approx (5\text{–}10)D_{\tau 1}$.

One should note that to derive the criteria (46)–(50) analytically we have made several assumptions concerning the

phase matching ($n_\omega^{(0)} = n_{2\omega}^{(0)} = n$), equality of nonlinear coefficients $\chi_\omega^{(0)} = \chi_{2\omega}^{(0)} = \chi$, and fulfillment of (5). Through normalization these assumptions result in $D_{x1} = 2D_{x2}$ and $D_{\tau 2} = 2D_{\tau 1}$. Moreover, to simplify the interpretation for numerical results we suppose that dimensionless soliton spatial and temporal widths $\bar{R}_0 = \bar{\tau}_0 = 1$. Hence, we arrive at the following form of the dimensionless coefficient μ introduced in (45):

$$\mu = \frac{2\varepsilon_d}{D_{\tau 1}\varepsilon_w}(4D_{q1} + D_{q2}). \tag{59}$$

Besides that, we can express the periods of spatial oscillations (53) in dimensionless form as well. The dimensionless period of spatial oscillations in the absence of waveguide T_0 is

$$T_0 = \pi\sqrt{\frac{3}{\varepsilon_d D_{\tau 1} D_{x1}}}. \tag{60}$$

The ratio of dispersion an diffraction lengths included in (46)–(50) and (52) in dimensionless form looks like

$$\frac{l_d}{l_D} = \frac{2D_{x1}\varepsilon_d}{D_{\tau 1}}. \tag{61}$$

To investigate numerically the regimes of the formation and propagation of two-component optical bullets we approximate (54) by a conservative difference scheme based on the Crank-Nicolson method. This method guarantees the preservation of difference analogues of the integrals (55), (56). To compute the solution on the next layer along the propagation coordinate we use a multistep effective iterative solver [14]. This method allows us to carry out an accurate and efficient modeling of the investigated processes. Implementing calculations, we usually take a limited computational domain in transverse directions $\bar{x}$ and $\bar{\tau}$:

$$-L_x/2 < \bar{x} < L_x/2, \quad -L_\tau/2 < \bar{\tau} < L_\tau/2,$$

where L_x and L_τ are chosen so that the amplitudes of both harmonics decay to zero at the boundaries of this domain. In particular cases, when L_x and L_τ are too large, the efficiency of the method can be improved by using absorbing boundary conditions along the coordinates $\bar{x}$ and $\bar{\tau}$. To this end we embed an artificial absorption in the system (54) [14].

Our numerical experiment is divided into three series. In the first series we consistently investigate in detail a two-component light bullet propagation provided phase matching. In this series we launch both input pulses of the forms (57) and (58). In the second series we calculate and discuss some examples with phase mismatching. In the final series of numerical simulation we consider a waveguide at one frequency only.

Let us start with the first series of computations. We suppose that the phase matching condition is satisfied ($\Delta\bar{k} = 0$) and check the criteria (46)–(50) and (44). We simulate the propagation of a two-component light bullet (57) when the problem parameters are chosen close to the limit of the fulfillment of the criteria (46)–(50). To verify that two pulses form stable parametric solitons, we pay special attention to the conservativeness of the generalized phase $\Phi = 2\varphi_1 - \varphi_2$. It is known that the generalized phase has a constant value for parametric solitons [12].

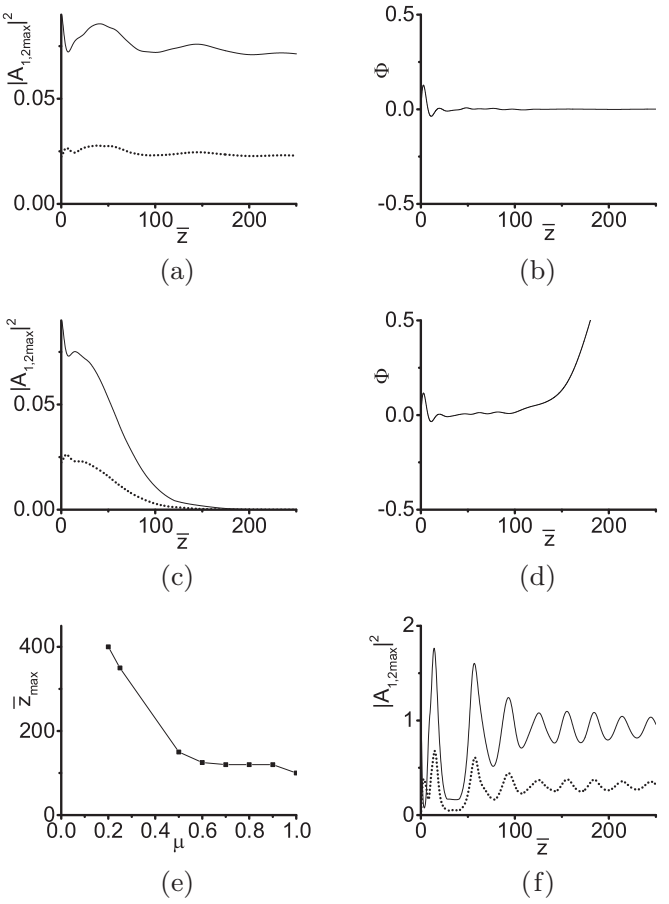

FIG. 3. Anomalous dispersion and defocusing waveguide at phase matching. Peak intensities of the fundamental (solid line) and second (dotted line) harmonics vs the propagation distance (a, c). Generalized phase (b, d). $\mu = 0.2$, $D_{q1} = 0.0017$, $D_{q2} = 0.0034$, $D_{x1} = 0.112$, $D_{x2} = 0.056$, $D_{\tau 1} = -0.1$, $D_{\tau 2} = -0.2$, $E = 0.3$, $\gamma = 0.5$ (a, b) and $\mu = 0.5$, $D_{q1} = 0.0042$, $D_{q2} = 0.0084$, $D_{x1} = 0.1$, $D_{x2} = 0.05$, $D_{\tau 1} = -0.1$, $D_{\tau 2} = -0.2$, $E = 0.3$, $\gamma = 0.5$ (c, d). Dependence of the distance $\bar{z}_{max}$ at which the phase behavior abruptly deviates from the quasisoliton regime on μ (e). In (e) from (46), (48), and (61) $D_{x1} = 2(\mu - 3)D_{\tau 1}/5$, $D_{x2} = D_{x1}/2$, $D_{q1} = \mu D_{\tau 1}/12$, $D_{q2} = 2D_{q1}$; other parameters are the same as in (a)–(d). Input pulses of the form (57) at both frequencies. The same as in (a) at SHG, $E = 1.0$ (f).

Below we consistently discuss the numerical simulation of three cases considered in the previous section.

d. Anomalous GVD, defocusing waveguide ($D_{\tau 1,2} < 0$, $\varepsilon_d = -1$, $\varepsilon_w = +1$). The principal interest in this case is to refine the limits of the dimensionless criteria (46) and (48) rewritten by taking into account (61). One should note that a combination of the mentioned criteria gives $0 < \mu < 1$.

Figures 3(a)–3(d) show the dependencies of peak intensities and generalized phase on propagation coordinate $\bar{z}$ for both harmonics. Figures 3(a) and 3(b) correspond to $\mu = 0.2$. Numerical simulation demonstrates that after a short initial period the two-component light bullet propagates without distortions along the entire distance of computations. We reveal that there is no energy exchange between the fundamental and second harmonics: the maxima and minima of the

fundamental wave intensity coincide with those of the second harmonic intensity. This means that the regime of classic parametric solitons is established. This regime is known as a reactive one, and an optimal relation between phases of interacting waves is a characteristic sign of it [30]. Figure 3(b) illustrates the dependence of the generalized phase Φ on the distance $\bar{z}$ at the center of the $(\bar{x}, \bar{\tau})$ domain. We observe that after $\bar{z} \approx 40$ the generalized phase becomes constant. Thus, we confirm the stability of the derived soliton solution (51).

Then we increase the strength of the defocusing waveguide and investigate the case $\mu = 0.5$ [Figs. 3(c) and 3(d)]. Numerical simulation shows that, as in the previous case, the intensities of the fundamental and second harmonics change in-phase but there is energy dissipation and light bullet distortion [Fig. 3(c)]. We find out that there is an optimal relation between phases of interacting waves up to $\bar{z} = 100$ [Fig. 3(d)], confirming the stable propagation of the light bullet.

The generalization of our studies for an anomalous GVD, defocusing waveguide at phase matching is depicted in Fig. 3(e). Here we demonstrate the influence of μ on the distance $\bar{z}_{\max}$ at which the phase behavior abruptly deviates from the quasisoliton regime. From (46) we have $D_{x1} = 2(\mu - 3)D_{\tau 1}/5$, provided $D_{x2} = D_{x1}/2$, $D_{q1} = \mu D_{\tau 1}/12$, $D_{q2} = 2D_{q1}$. Other parameters are the same as in Figs. 3(a)–3(d). The input pulse has the form (57). It is necessary to underline that with increasing μ up to $\mu = 1$ we observe that the distance of stable two-component light bullet propagation decreases. For $\mu > 1$ the graph for generalized phase has no constant parts. Therefore, one should note the fulfillment of the criteria (46) combined with (61).

As mentioned above, the question of the possibility of generating a bullet, in particular, in the case under consideration, is rather essential. Figure 3(f) illustrates results of the computations when launching a pulse (58) at the fundamental frequency only. We observe significant fluctuations in the intensities of both harmonics during the initial energy exchange up to $\bar{z} = 100$. For a longer distance oscillations characterizing a stable bound state occur. It means the formation of a light bullet.

e. Anomalous GVD, focusing waveguide ($D_{\tau 1,2} < 0$, $\varepsilon_d = -1$, $\varepsilon_w = -1$). As shown recently in [12], a stable two-component light bullet may form in this case even without a waveguide. It is clear that the presence of a focusing waveguide strengthens this effect. There are no additional restrictions on parameters. Since $\mu > 0$, we get $D_{x1} > 6D_{\tau 1}/5$.

Figure 4, which shows dependencies of peak intensities and generalized phase on propagation coordinate $\bar{z}$ for both harmonics, illustrates stable quasisoliton propagation up to $\bar{z} = 500$. We remind the reader that in the absence of a waveguide "breathing" light bullets are observed in a quadratic nonlinear medium with anomalous dispersion [12,13]. All parameters of such bullets oscillate like harmonic functions. Waveguide introduction complicates the whole picture since additional oscillations caused by the waveguide appear. In general, the character of oscillations remains "breathing" but regular, with good coincidence between the period of oscillations predicted theoretically, $T \approx 33.5$, and the period of oscillations obtained in the numerical experiment, $T_{\exp} \approx 38.5$. As in the previous case, there is no energy exchange between the fundamental and second harmonics, the reactive regime is established.

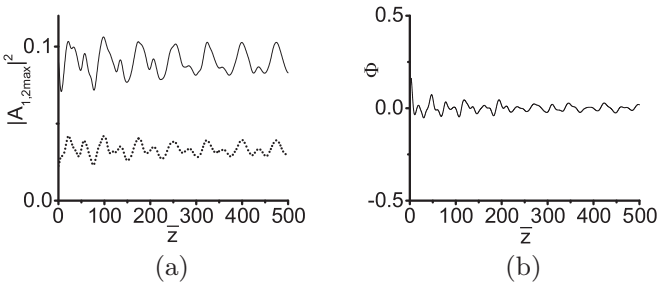

FIG. 4. Anomalous dispersion and focusing waveguide at phase matching. Peak intensities of the fundamental (solid line) and second (dotted line) harmonics vs the propagation distance (a). Generalized phase (b). Input pulses of the form (35) at both frequencies. $D_{q1} = -0.00625$, $D_{q2} = 0.0125$, $D_{x1} = 0.15$, $D_{x2} = 0.075$, $D_{\tau 1} = -0.1$, $D_{\tau 2} = -0.2$, $E = 0.3$, $\gamma = 0.5$.

We also carried out computations in the regime of SHG in this case. Launching a signal of the form (58) in the numerical experiment, we demonstrate that in the focusing waveguide at anomalous dispersion a spatiotemporal bullet forms and robustly propagates.

f. Normal GVD, focusing waveguide ($D_{\tau 1,2} > 0$, $\varepsilon_d = +1$, $\varepsilon_w = -1$). There are no additional restrictions on parameters. Since $D_{x1} > 0$ and $D_{\tau 1,2} > 0$, $\mu > 3$. If $\mu \to 3$, the diffraction coefficient $D_{x1} \to 0$. Thus, we deal with wider (shortwave) beams.

First we discuss the case when the value of μ is far from the limit determined by (26c). Figure 5 corresponds to $\mu = 10$ and illustrates z dependencies of the calculated peak amplitudes (a), generalized phase (b) and temporal and spatial widths (c, d) of both harmonics. The calculated profiles are compared with those of the form (8a) having the same amplitudes, widths, and durations at the center of the beam pulse [Figs. 5(e) and 5(f)]. A similar comparison of the calculated and analytical profiles of both harmonics at the distance $\bar{x} = 1$ from the beam-pulse center is given in Fig. 5(g). One can see quite a good match between the analytical prediction and the calculated profiles. The profiles calculated numerically demonstrate a good coincidence with the theoretical solution applied in accordance with the above-described method. Moreover, there is an agreement between the period of oscillations predicted theoretically, $T \approx 10.8$, and the period of oscillations obtained in the numerical experiment, $T_{\exp} \approx 10.8$. Therefore, one may conclude that the trial functions (51) are chosen correctly.

It is important to underline that in the absence of a waveguide, provided there is normal dispersion, both pulses of the fundamental and second harmonics are unstable and light bullets cannot form. Localizations in the form of bullets are observed only in a waveguide.

Figure 6 demonstrates the behavior of the two-component bullet when μ is closer to the limit. Figures 6(a) and 6(b) show dependencies of peak intensities and generalized phase on propagation coordinate $\bar{z}$ for both harmonics at $\mu = 6$. The period of oscillations predicted theoretically, $T \approx 22.2$, is still close to that obtained in numerical experiment, $T_{\exp} \approx 22$.

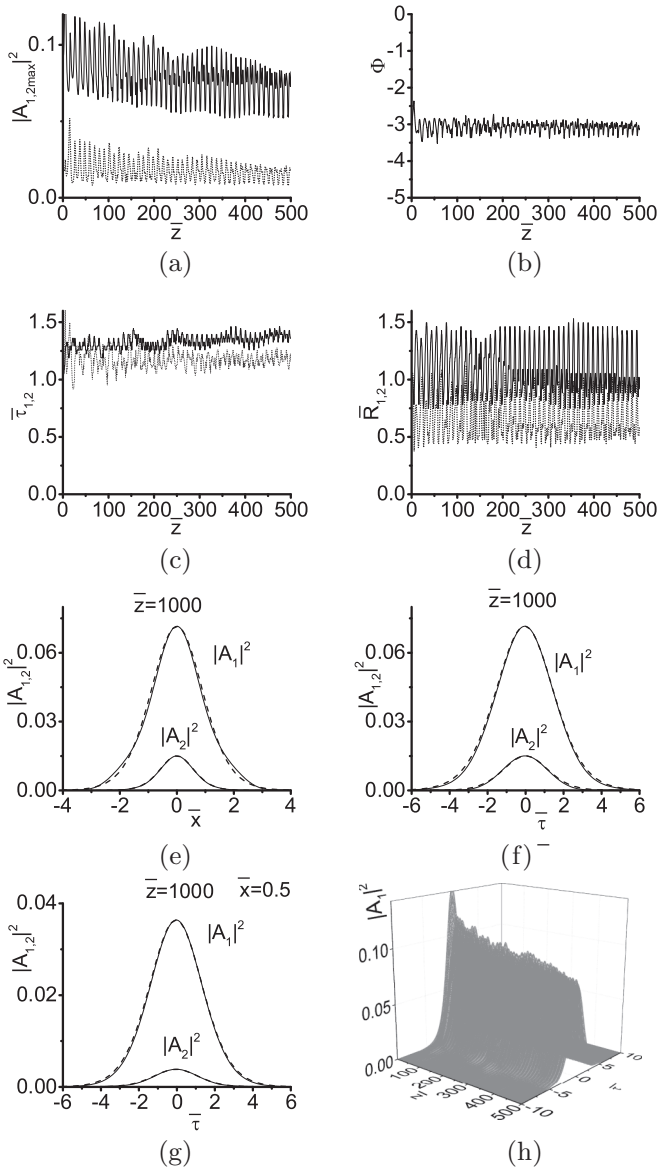

FIG. 5. Normal dispersion and focusing waveguide at phase matching. Dependencies of the calculated peak amplitudes (a), generalized phase (b), and temporal and spatial widths (c, d) of the fundamental (solid lines) and second (dotted lines) harmonics. Transversal temporal (e) and spatial (f) profiles of both harmonics calculated at the distance $\bar{z} = 1000$ from the beam-pulse center (solid lines) compared with the approximations of the form (51) of the maximum intensity and temporal and spatial widths of the calculated first and second harmonics (dashed lines). Similar comparison of the calculated and analytical profiles of both harmonics at the same distance from the beam-pulse center (g). Propagation of the beam pulse (h). Input pulses of the form (35) at both frequencies. $\mu = 10$, $D_{q1} = -0.083$, $D_{q2} = -0.166$, $D_{x1} = 0.28$, $D_{x2} = 0.14$, $D_{\tau 1} = 0.1$, $D_{\tau 2} = 0.2$, $E = 0.3$, $\gamma = 0.5$.

One may conclude that a quasisoliton regime establishes after $\bar{z} = 200$, approximately. Further decrease of μ changes the picture. Figures 6(c) and 6(d) show dependencies of peak intensities and generalized phase on propagation coordinate $\bar{z}$ for both harmonics at $\mu = 5$. Oscillations become less regular; the predicted oscillation period $T \approx 30.5$ differs from

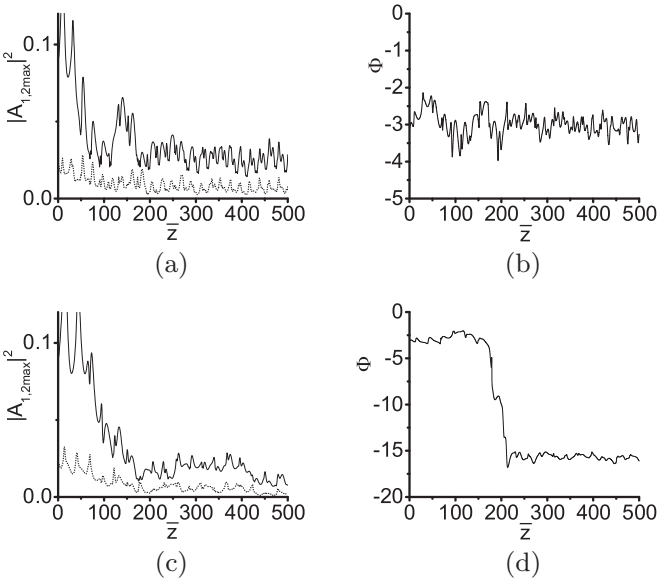

FIG. 6. Normal dispersion and focusing waveguide at phase matching. Parameters are close to the limits of the criterion (26c). Dependencies of the calculated peak amplitudes (first harmonic: solid lines; second one: dotted lines) and generalized phase at $\mu = 6$, $D_{q1} = -0.05$, $D_{q2} = -0.1$, $D_{x1} = 0.12$, $D_{x2} = 0.06$, $D_{\tau 1} = 0.1$, $D_{\tau 2} = 0.2$, $E = 0.3$, $\gamma = 0.5$ (a,b) and at $\mu = 5$, $D_{q1} = -0.042$, $D_{q2} = -0.084$, $D_{x1} = 0.08$, $D_{x2} = 0.04$, $D_{\tau 1} = 0.1$, $D_{\tau 2} = 0.2$, $E = 0.3$ (c,d).

that obtained in the numerical experiment, $T_{\text{exp}} \approx 27$, by 10%. But it is still possible to talk about the quasistable propagation of a two-component light bullet after $\bar{z} = 200$, approximately, since the generalized phase oscillates near a certain averaged value.

It is rather important that in our calculations snake instability does not arise, and the solution agrees well with the analytical one. This confirms the second part of the analysis, where such instability is not taken into account because it appears to be suppressed by focusing the waveguide effect at normal GVD.

Then we focus on the process of optical bullet generation from a powerful fundamental beam at phase matching and normal dispersion. One should note that bullet generation at

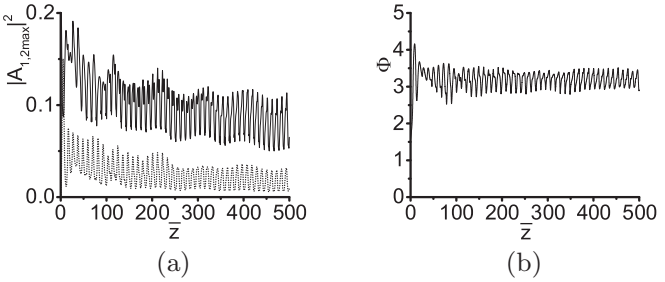

FIG. 7. Normal dispersion and focusing waveguide at phase matching. Dependencies of the calculated peak amplitudes (first harmonic: solid line; second one: dotted line) (a) and generalized phase (b) at SHG. $\mu = 10$, $D_{q1} = -0.083$, $D_{q2} = -0.166$, $D_{x1} = 0.28$, $D_{x2} = 0.14$, $D_{\tau 1} = 0.1$, $D_{\tau 2} = 0.2$, $E = 0.5$, $\gamma = 0.5$.

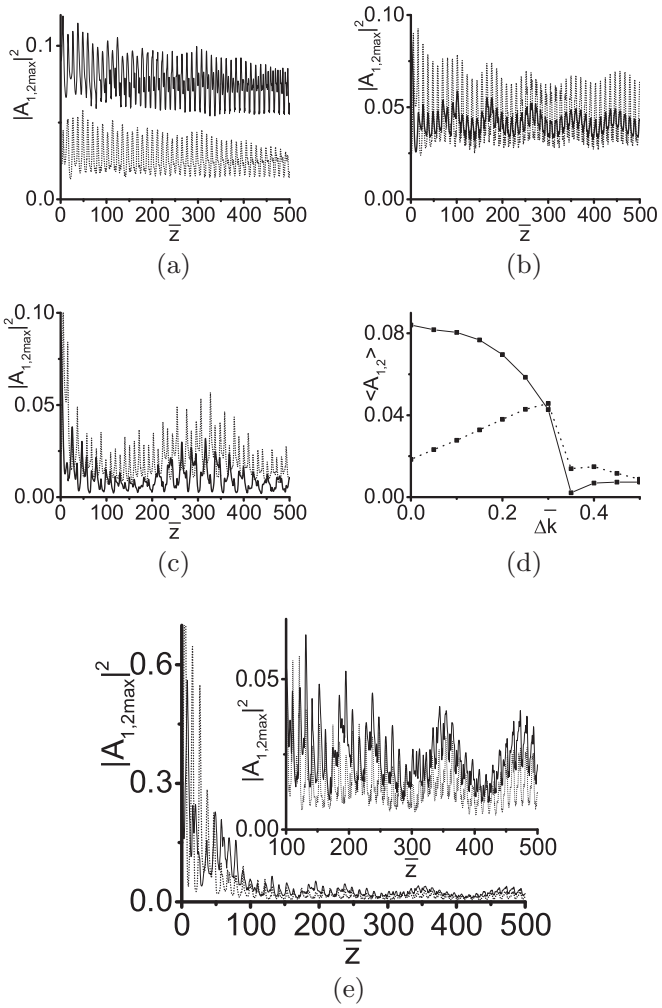

FIG. 8. Normal dispersion and focusing waveguide at phase mismatching. Input pulses of the form (57), $\mu = 10$, $D_{q1} = -0.083$, $D_{q2} = -0.166$, $D_{x1} = 0.28$, $D_{x2} = 0.14$, $D_{\tau 1} = 0.1$, $D_{\tau 2} = 0.2$, $E = 0.3$, $\gamma = 0.5$. Dependencies on $\bar{z}$ of the calculated peak amplitudes (first harmonic: solid lines; second one: dotted lines). $\Delta\bar{k} = 0.1$ (a), $\Delta\bar{k} = 0.3$ (b), $\Delta\bar{k} = 0.4$ (c); dependencies on $\Delta\bar{k}$ of the maximum amplitudes of the fundamental (solid line) and second (dotted line) harmonics in time and transversal coordinate, which are averaged over the distance from $\bar{z} = 100$ to $\bar{z} = 200$ (d). Input pulse of the form (58) at the fundamental frequency, $\Delta\bar{k} = 0.2$, $E = 1.0$; the inset shows the propagation of the formed bullet at a larger scale (e).

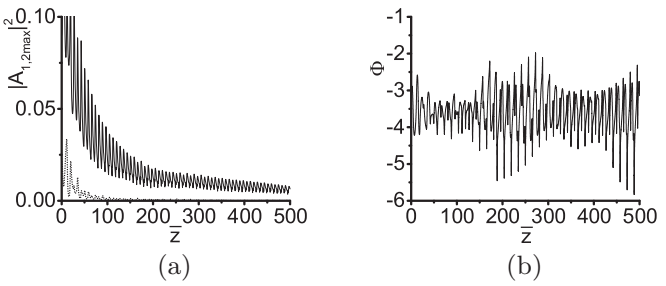

FIG. 9. Normal dispersion and focusing waveguide at the fundamental frequency only, $\Delta\bar{k} = 0$. Input pulses of the form (57) at both frequencies. Dependencies of the calculated peak amplitudes (first harmonic: solid line; second one: dotted line) (a) and generalized phase (b). $D_{q1} = -0.15$, $D_{q2} = -0.0$, $D_{x1} = 0.28$, $D_{x2} = 0.14$, $D_{\tau 1} = 0.1$, $D_{\tau 2} = 0.2$, $E = 0.3$, $\gamma = 0.5$.

anomalous dispersion was demonstrated earlier in [12]. In the present computations we launch the initial pulse at the fundamental frequency only in the form (58). Figures 7(a) and 7(b) show the dependencies of peak intensities and generalized phase on propagation coordinate $\bar{z}$ for both harmonics. One should note that at the first propagation stage, when the second harmonic is generating and a two-component bullet is forming, there are intensive variations of the peak intensity and generalized phase. These are caused by initial energy exchange transformed into the reactive regime of wave interaction. At far distances, a solitonlike profile forms. This process is again accompanied by strong variations of the peak intensity but the generalized phase actually becomes constant. Therefore, it is demonstrated that the stable two-component light bullet forms in this case.

We proceed with the second series of computations. Now we suppose that the phase matching condition is violated. Figure 8 demonstrates the behavior of the two-component bullet in a focusing waveguide at normal dispersion and weak phase mismatching. We see that small values of $\Delta\bar{k}$ do not interrupt the process of two-component light bullet propagation: oscillations near some averaged value have regular character. We reveal that $\Delta\bar{k} = 0.4$ is a critical value. As soon as dimensionless mismatching passes it, the light bullet stable propagation is violated. We note a good coincidence of the theoretical and experimental periods in this case.

It is remarkable that we have managed to get a steady-state two-color bullet at a certain phase mismatching in the regime of SHG. In Fig. 8(d) we see a sharp intensity drop in the initial propagation stage. It is obviously due to energy transfer to the second harmonic and dissipation as well. But beginning from the distance $\bar{z} = 100$ it is possible to talk about the propagation of a steady-state soliton.

The final series of our modeling demonstrates that in accordance with the theoretical assumption a two-component light bullet may form at normal dispersion when an effective waveguide exists only for the fundamental harmonic. Figure 9 shows that the second harmonic pulse is also captured in a waveguide and then a quasisoliton propagation takes place. Significant dissipation of energy and intensive generalized phase oscillations are characteristic in this case. However, the beam profile preserves its shape for dozens of dispersion and diffraction lengths.

When an effective waveguide exists only for the second harmonic pulse, quasistable propagation is too short: no more than one dispersion or diffraction length. Later a two-component light bullet breaks down.

Our computations also demonstrate that a two-component bullet may form and propagate at a certain distance in the regime of SHG if the focusing waveguide is at the fundamental frequency only.

V. CONCLUSION

Application of the AL method to the system of spatiotemporal parabolic equations describing the process of SHG in a planar waveguide yields an asymptotic analytical solitary-wave solution in the form of a two-component light bullet. Bullet formation is possible in the following three cases: anomalous GVD, defocusing waveguide; anomalous GVD, focusing waveguide; and normal GVD, focusing waveguide. We highlight the remarkable fact that, in contrast to a homogeneous medium, the waveguide geometry allows us to observe stable two-component light bullets in media with weak normal dispersion which corresponds to defocusing nonlinearity.

The bullet manifests a "breathing" character. Propagating along the longitudinal coordinate, it undergoes regular oscillations of intensities, temporal and transversal widths, etc.

We verify the results obtained with the help of the AL method by direct numerical simulation. Taking the derived analytical solution as initial condition, we show a good agreement between the analytical estimations and numerical results. A stable propagation of light bullets either at anomalous or at normal dispersion is confirmed by computations. We also verify and refine the analytical criteria of stable bullet propagation in a planar waveguide at anomalous GVD with defocusing waveguide and normal GVD with focusing waveguide.

In a focusing waveguide at anomalous GVD two-color light bullets are unconditionally stable, provided there is a certain parameter coherence.

We numerically investigate a possibility of soliton existence at the presence of phase mismatch. We found critical mismatch values below which light bullets can be formed and propagate robustly. Above the thresholds we show the broadening of both pulses.

We analytically predict and numerically confirm a possibility of light bullet stable propagation at normal group velocity dispersion, when the focusing waveguide is only at one frequency.

Our numerical experiments confirm the conclusion of [27] that a focusing waveguide effectively suppresses the development of snake instability. This, in particular, makes it possible to form a light bullet in a focusing waveguide in the region of normal group velocity dispersion.

Earlier we demonstrated the generation of a two-color light bullet at SHG at anomalous dispersion. Optical bullet generation from a powerful fundamental beam at phase matching or mismatching and normal dispersion is a focus of the present study.

Further studies should include the expansion for volumetric waveguides starting from the axially symmetric ones. Moreover, it is reasonable to take into account dependencies of nonlinear susceptibilities on waveguide transversal coordinates.

ACKNOWLEDGMENT

This work is supported by the Russian Science Foundation (Project No. 17-11-01157).

[1] Y. S. Kivshar and G. Agrawal, *Optical Solitons: From Fibers to Photonic Crystals* (Academic, San Diego, 2003).
[2] A. B. Aceves, Chaos **10**, 584 (2000).
[3] T. Iizuka and Y. S. Kivshar, Phys. Rev. E **59**, 7148 (1999).
[4] C. Conti, G. Assanto, and S. Trillo, Opt. Express **3**, 389 (1998).
[5] K. Zhan, H. Tian, X. Li, X. Xu, Z. Jiao, and Y. Jia, Sci. Rep. **6**, 32990 (2016).
[6] O. V. Borovkova, Y. V. Kartashov, V. A. Vysloukh, V. E. Lobanov, B. A. Malomed, and L. Torner, Opt. Express **20**, 2657 (2012).
[7] Y. Wang and S. Zhou, AIP Adv. **7**, 085006 (2017).
[8] S. G. Ali, B. Talukdar, and S. Roy, Acta Phys. Pol. A **111**, 289 (2007).
[9] W. B.Cardoso, H. L. C. Couto, A. T. Avelar, and D. Bazeia, Commun. Nonlinear Sci. Numer. Simul. **48**, 474 (2017).
[10] Y. Kong, Opt. Commun. **371**, 27 (2016).
[11] W.-J. Liu, B. Tian, T. Xu, K. Sun, and Y. Jiang, Ann. Phys. (NY) **325**, 1633 (2010).
[12] S. V. Sazonov, M. S. Mamaikin, M. V. Komissarova, and I. G. Zakharova, Phys. Rev. E **96**, 022208 (2017).
[13] S. V. Sazonov, M. S. Mamaikin, I. G. Zakharova, and M. V. Komissarova, Phys. Wave Phenom. **25**, 83 (2017).
[14] I. G. Zakharova, A. A. Kalinovich, M. V. Komissarova, and S. V. Sazonov, in *Finite Difference Methods. Theory and Applications*, edited by I. Dimov, I. Faragó, and L. Vulkov, Lecture Notes in Computer Science Vol. 11386 (Springer, Cham, Switzerland, 2019), p. 670.
[15] S. K. Zhdanov and B. A. Trubnikov, Zh. Eksp. Teor. Fiz. **92**, 1612 (1987) [Sov. Phys. JETP **65**, 904 (1987)].
[16] D. Anderson, M. Desaix, M. Lisak, and M. L. Quiroga-Teixeiro, J. Opt. Soc. Am. B **9**, 1358 (1992).
[17] S. V. Sazonov, J. Exp. Theor. Phys. **103**, 126 (2006).
[18] Y. N. Karamzin and A. Sukhorukov, Zh. Eksp. Teor. Fiz. **68**, 834 (1975) [Sov. Phys. JETP **41**, 414 (1975)].
[19] M. Born and E. Wolf, *Principles of Optics* (Pergamon, New York, 1968).
[20] S. V. Sazonov, Opt. Spectrosc. **79**, 260 (1995).
[21] E. A. Kuznetsov, A. M. Rubenchik, and V. E. Zakharov, Phys. Rep. **142**, 103 (1986).
[22] Y. S. Kivshar and D. E. Pelinovsky, Phys. Rep. **331**, 117 (2000).
[23] B. A. Malomed, D. Mihalache, F. Wise, and L. Torner, J. Opt. B: Quantum Semiclassical Opt. **7**, R53 (2005).
[24] V. E. Zakharov and A. M. Rubenchik, Zh. Eksp. Teor. Fiz. **65**, 99 (1973) [Sov. Phys. JETP **38**, 494 (1974)].
[25] D. E. Pelinovsky, Math. Comput. Simul. **55**, 585 (2001).
[26] G. Lombardi, W. Van Alphen, S. N. Klimin, and J. Tempere, Phys. Rev. A **96**, 033609 (2017).
[27] L. A. Cisneros-Ake, R. Carretero-González, P. G. Kevrekidis, and B. A. Malomed, Commun. Nonlinear Sci. Numer. Simul. **74**, 268 (2019).
[28] D. R. Tilley and J. Tilley, *Superfluidity and Superconductivity* (Van Nostrand Reinhold, New York, 1974).

[29] E. M. Lifshitz and L. P. Pitaevskii, *Statistical Physics, Part 2: Theory of the Condensed State*, Course of Theoretical Physics Vol. 9 (Butterworth-Heinemann, New York, 1980).

[30] S. A. Akhmanov, A. P. Sukhorukov, and R. V. Khokhlov, Sov. Phys. Usp. **10**, 609 (1968).

[31] S. V. Sazonov, J. Phys. Soc. Jpn. **85**, 124404 (2016).

[32] O. V. Shtyrina, M. P. Fedoruk, Y. S. Kivshar, and S. K. Turitsyn, Phys. Rev. A **97**, 013841 (2018).

[33] K. Rypdal and J. J. Rasmussen, Phys. Scr. **40**, 192 (1989).

[34] A. A. Kanashov and A. M. Rubenchik, Physica D **4**, 122 (1981).